

## 냉간가공과 베타급냉된 Zr-Sn 합금의 재결정 거동

이 명 호 · 정 용 환

지르코늄 핵연료피복관 개발팀 한국원자력연구소

### Recrystallization Behavior of Cold-worked and $\beta$ -Quenched Zr-Sn Alloys

Myung-Ho Lee and Yong-Hwan Jeong

Advanced Zr Alloy Development,

Korea Atomic Energy Research Institute, Taejon 305-353, Korea

(2000년 6월 29일 받음, 2000년 8월 28일 최종수정본 받음)

**초 록** 냉간가공과 베타급냉된 Zr-Sn 합금의 재결정 거동을 미소경도 시험과 미세 조직 관찰 방법에 의해서 조사하였다. 베타급냉 처리된 합금의 재결정은 냉간가공된 합금의 재결정보다 늦게 일어났는데, 이는 냉간 가공에 의해 도입된 축적에너지가 더 높다는 것을 의미한다. 냉간가공제와 베타급냉제의 초기 경도는 동일할지라도 재결정거동은 아주 다르게 나타났다. TEM 조직관찰 결과를 근거로 할 때, 냉간가공제는 subgrain합체에 의해서 재결정이 일어나며 베타급냉제는 응력유기 입계이동에 의해서 재결정이 일어나는 것으로 밝혀졌다.

**Abstract** Recrystallization behaviors of cold-worked and  $\beta$ -quenched Zr-Sn alloys were investigated by the micro-hardness tests and microscopic examinations. The recrystallization of the  $\beta$ -quenched alloys was retarded in comparison with that of the cold-worked alloys, suggesting that the stored energy of the cold-worked alloys is larger than that of the  $\beta$ -quenched alloys. Although initial hardness for the cold-worked and the  $\beta$ -quenched specimens had an equal value, the recrystallization behaviors were observed to be quite different. Based on the transmission electron microscope (TEM) studies, it was suggested that the recrystallization of the cold-worked specimen would have occurred by subgrain coalescence while that of the  $\beta$ -quenched specimen by strain-induced grain boundary migration.

**Key words** : recrystallization, Zr alloys, annealing, hardness, subgrain

### 1. INTRODUCTION

Since nuclear fuel cladding is used in hot, pressurized, and irradiated conditions, many properties such as low thermal neutron capture cross section, high resistance to corrosion in high temperature water, and relatively high mechanical strength should meet the requirements for the cladding. The corrosion resistance of the properties is particularly important because the cladding is exposed to the very corrosive environment. Zr metal has been selected as the cladding material because it has low thermal neutron capture cross section that is about 30 times less than that of stainless steel.<sup>1)</sup> A great deal of researches had been carried out to improve the corrosion resistance and mechanical properties of the cladding material. After the additions of a small amount of Sn, Fe, and Cr in Zr matrix were found to be effective in improving the corrosion resistance of the cladding under PWR (pressurized water reactor) operation conditions, Zircaloy-4 (Zr-1.5Sn-0.2Fe-0.1Cr) has been successfully used as clad-

ding material in PWR for many years. However, more advanced Zr-based alloys than Zircaloy-4 have been developed in many research groups<sup>2)</sup> to meet severer conditions such as high burnup, high operation temperature and high pH. When a new alloy is developed, an appropriate process condition should be established to optimize its properties since the corrosion and mechanical characteristics of the Zr-based alloys are very dependent on their chemical compositions and process conditions. It is also necessary to understand the recrystallization behavior of the alloy because the annealing treatment is always carried out during the manufacturing process. The final microstructure is often controlled (i.e., recrystallized, partially recrystallized, or stress relieved) according to the required properties. In Zr-Sn alloys, the Sn content has been reported to significantly affect the microstructure and corrosion resistance of alloys.<sup>3)</sup> Although the general effect of Sn on the microstructural change such as recrystallization during annealing was known, detailed information on the change is not available. Furthermore, the recryst-

stallization behavior in relation to the pre-treatment condition before annealing ( $\beta$ -quenched or cold-worked) has not been investigated. Since different recrystallization mechanisms might be involved depending on the characteristics of stressed structure, quite different behaviors could be observed of the recrystallization. In this study, the recrystallization behaviors of Zircaloy-4, Zr-0.5Sn, and Zr-1.5Sn alloys were investigated and the effect of the pre-treatment condition before annealing on the recrystallization was also evaluated. The recrystallization mechanisms for Zr-Sn alloys were suggested on the basis of the results of microscopic examination.

## 2. EXPERIMENTAL PROCEDURES

Zr-0.5Sn and Zr-1.5Sn alloys prepared in the laboratory and commercial Zircaloy-4 were prepared for this study. Zr-Sn alloy ingots (400g) were prepared by the vacuum arc remelting. The ingots were quenched into water ( $\beta$ -quenching heat treatment) after heating at 1050°C for 30 minutes to homogenize the chemical composition. And then hot rolling (60%) was carried out of the ingots after annealing at 700°C for 2 hours. Sheets with 1mm thickness were manufactured by cold rolling (50%). The  $\beta$ -quenching treatments were conducted again for some sheet specimens in order to make all the precipitates previously formed dissolve into matrix. Finally, the samples were annealed at different temperatures ranging from 300°C to 800°C for 1 hour. After finishing the final heat treatment, the test specimens were prepared for the polarized optical microscope studies by etching with a solution of HF 10%, HNO<sub>3</sub> 45% and H<sub>2</sub>O 45%. The microhardness tests were also carried out for those samples to characterize the recrystallization behavior. The microstructures of the samples were mainly investigated by a transmission electron microscope (TEM). The TEM specimens were prepared by mechanical grinding up to 60 $\mu$ m in thickness and twin-jet polishing in a solution of ethanol (90%) and perchloric acid at -45°C.

## 3. RESULTS AND DISCUSSION

### 3.1. Microhardness

The effect of annealing temperature on the microhardness of Zr-Sn alloys is shown in Fig. 1. The recrystallization behaviors of the alloys are compared for the cold-worked and the  $\beta$ -quenched conditions. In the case of cold-worked samples (in Fig. 1(a)) the microhardness remained almost constant up to 500°C and sharp drops occurred in the temperature range of

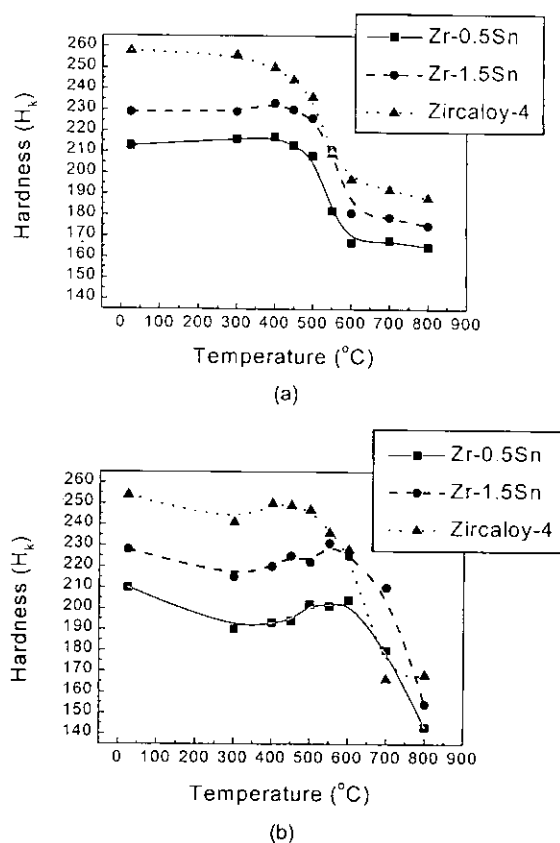


Fig. 1. Variations of Knoop hardness of Zr-based alloys (a) Cold-worked (b)  $\beta$ -quenched

500 to 600°C. The microhardness changes are shown to be more complicated in  $\beta$ -quenched alloys (in Fig. 1 (b)). The hardness slowly decreased at the beginning and then slightly increased. It is thought that the initial decrease in hardness at 300°C-400°C was due to recovery through the rearrangement of dislocation which introduced during quenching and the slight increase at 500°C was caused by the precipitation.<sup>4)</sup> Sn would not be detected in the precipitates because the solubility of Sn in  $\alpha$ -Zr is relatively high (about 2wt.%.<sup>5)</sup> But Fe and Cr, especially Fe, are usually present at a level of about 500 ppm in Zr metal as impurities and their solubilities in  $\alpha$ -Zr are very limited (hundreds ppm<sup>6)</sup> so that Fe and/or Cr precipitates usually form. The precipitates were found to consist of Zr, Fe, and Cr based on EDS in TEM.<sup>4)</sup> In the meantime, the start and finish temperatures of recrystallization for  $\beta$ -quenched alloys were observed to be relatively high as compared with that for the cold-worked specimen. This implies that the stored energy of the  $\beta$ -quenched alloys is smaller than that of the cold-worked alloys.

### 3.2. Microstructural changes

The typical microstructural changes during aging are shown in Figs. 2 and 3. In the case of the cold-worked

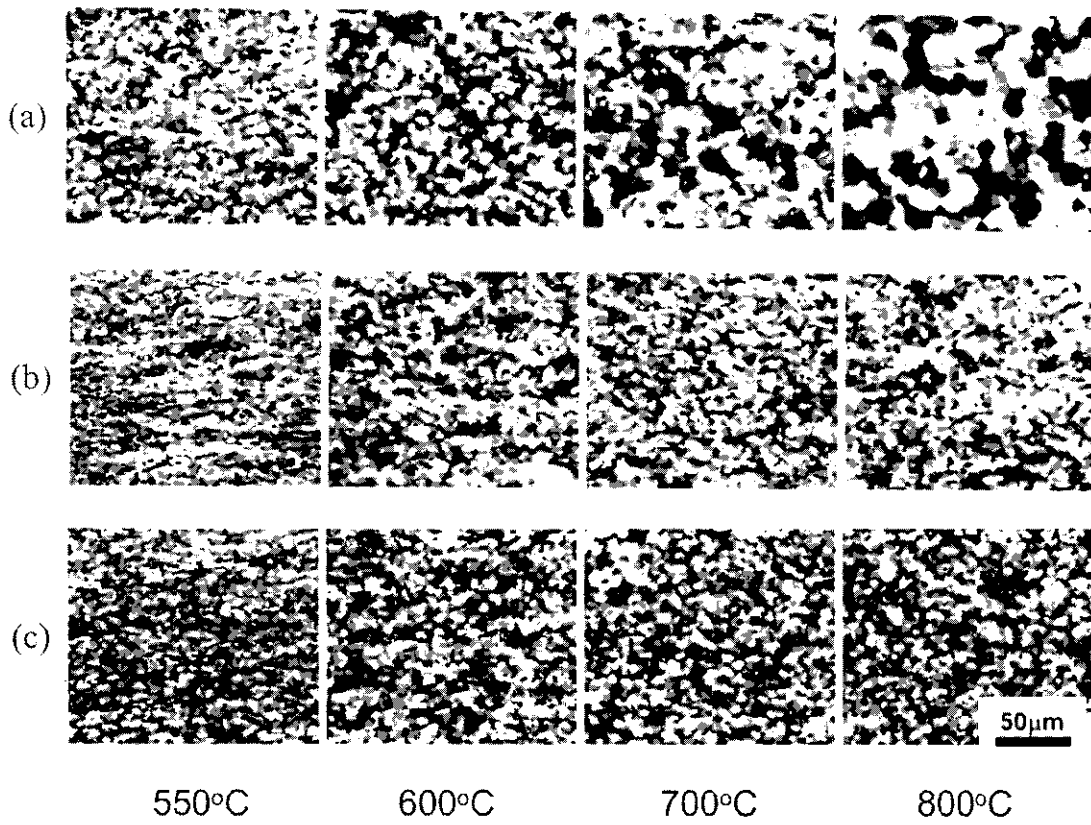


Fig. 2. Variations of the microstructures of cold-worked Zr-based alloys with annealing temperature for 1 hour (a) Zr-0.5Sn (b) Zr-1.5Sn (c) Zircaloy-4

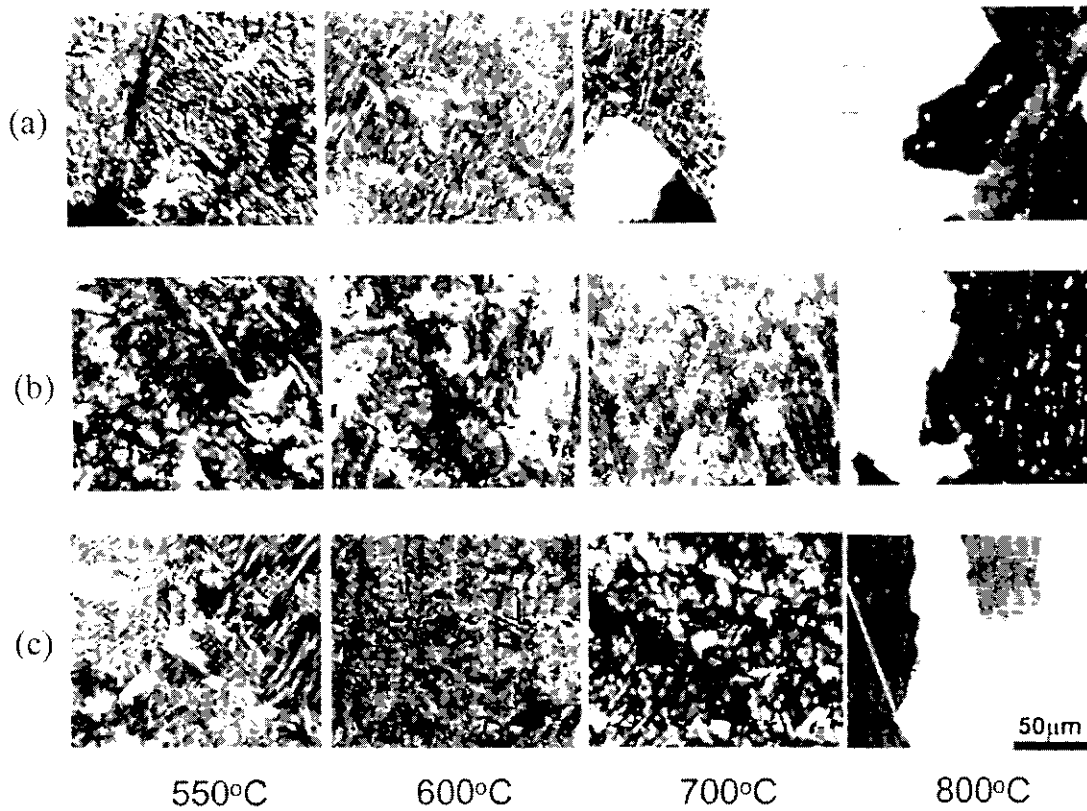


Fig. 3. Variations of the microstructures of  $\beta$ -quenched Zr-based alloys with annealing temperature for 1 hour (a) Zr-0.5Sn (b) Zr-1.5Sn (c) Zircaloy-4

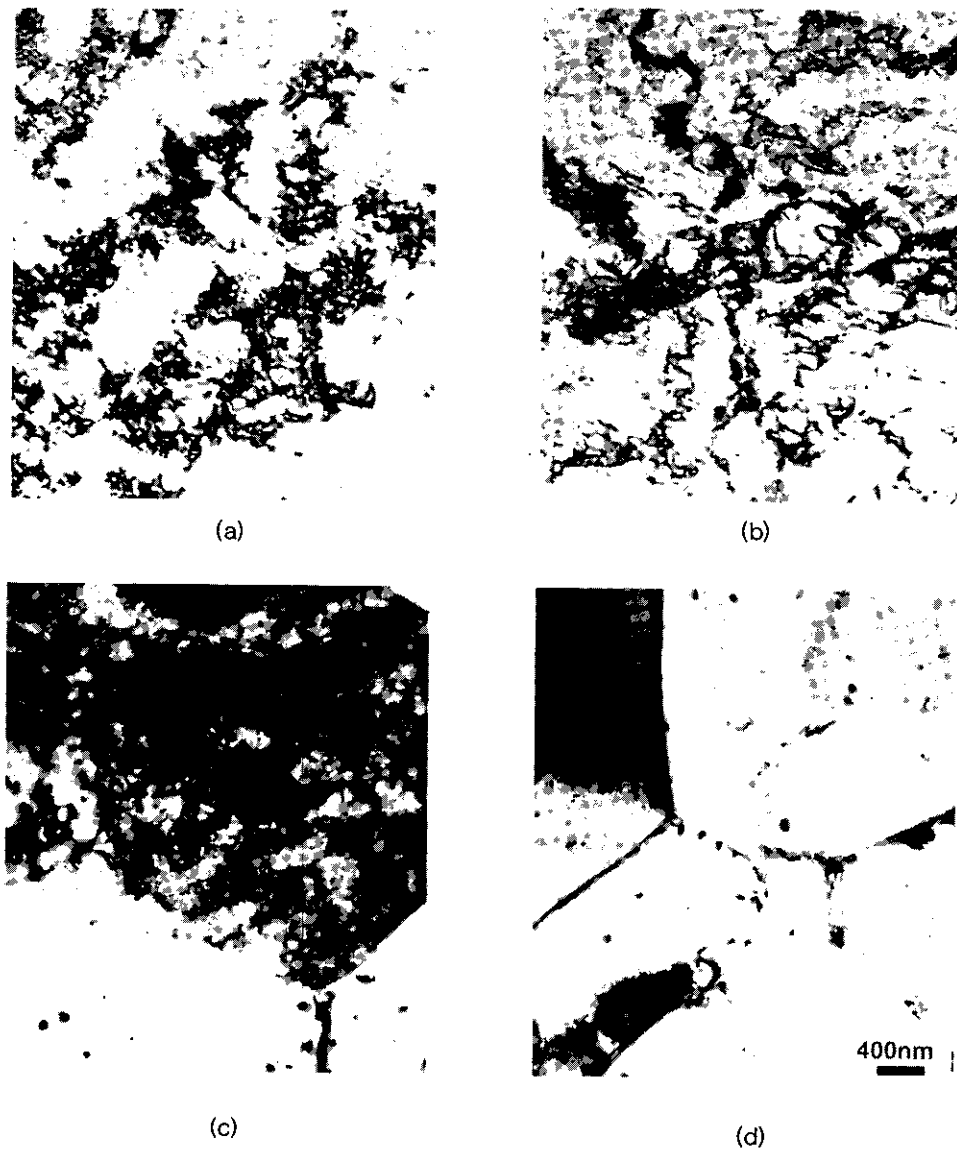


Fig. 4. Variations of microstructures of cold-worked Zr-1.5Sn alloy with annealing temperature (a) Room Temp. (b) 300°C (c) 550°C (d) 700°C

specimen (Fig. 2), the recrystallization of Zr-0.5Sn alloy was almost completed at 550°C for 1 hour while it was finished at 600°C in Zr-1.5Sn alloy and Zircaloy-4. In Zr-0.5Sn alloy, the grain growth phenomenon was also observed in high temperatures (700, 800°C) after recrystallization was finished. But it was not observed in Zr-1.5Sn alloy and Zircaloy-4. Fig. 3 shows the recrystallization of  $\beta$ -quenched samples. The martensite structure still remained up to 600°C and then new stress-free grains formed at higher temperatures. In Zr-0.5Sn alloy, the formation of those new grains occurred at about 700°C, but it was delayed to 800°C in Zr-1.5Sn alloy and Zircaloy-4. In conclusion, high Sn content is thought to delay the recrystallization process and to prohibit the grain growth. The detailed microstructural change during recrystallization can be

investigated by TEM and the micrographs for Zr-1.5Sn are shown in Figs 4 and 5. The typical dislocation cell structures caused by cold working were well observed in Fig. 4 (a) and (b). As the annealing temperature increased, the cell structure disappeared and new stress-free grains formed (in Fig. 4 (c)). At this temperature (550°C) the microhardness decreased sharply. And, as shown in Fig. 4 (d), all the dislocation cells disappeared completely and the recrystallization process was finished. Fig. 5 indicates the microstructural changes during the recrystallization of  $\beta$ -quenched samples. A martensite structure with fine plates and twins was observed in the samples aged at low temperatures. Some of dislocations within plates started to disappear at 550°C. As previously mentioned, microhardness increased at this temperature and this is thought to be due to the

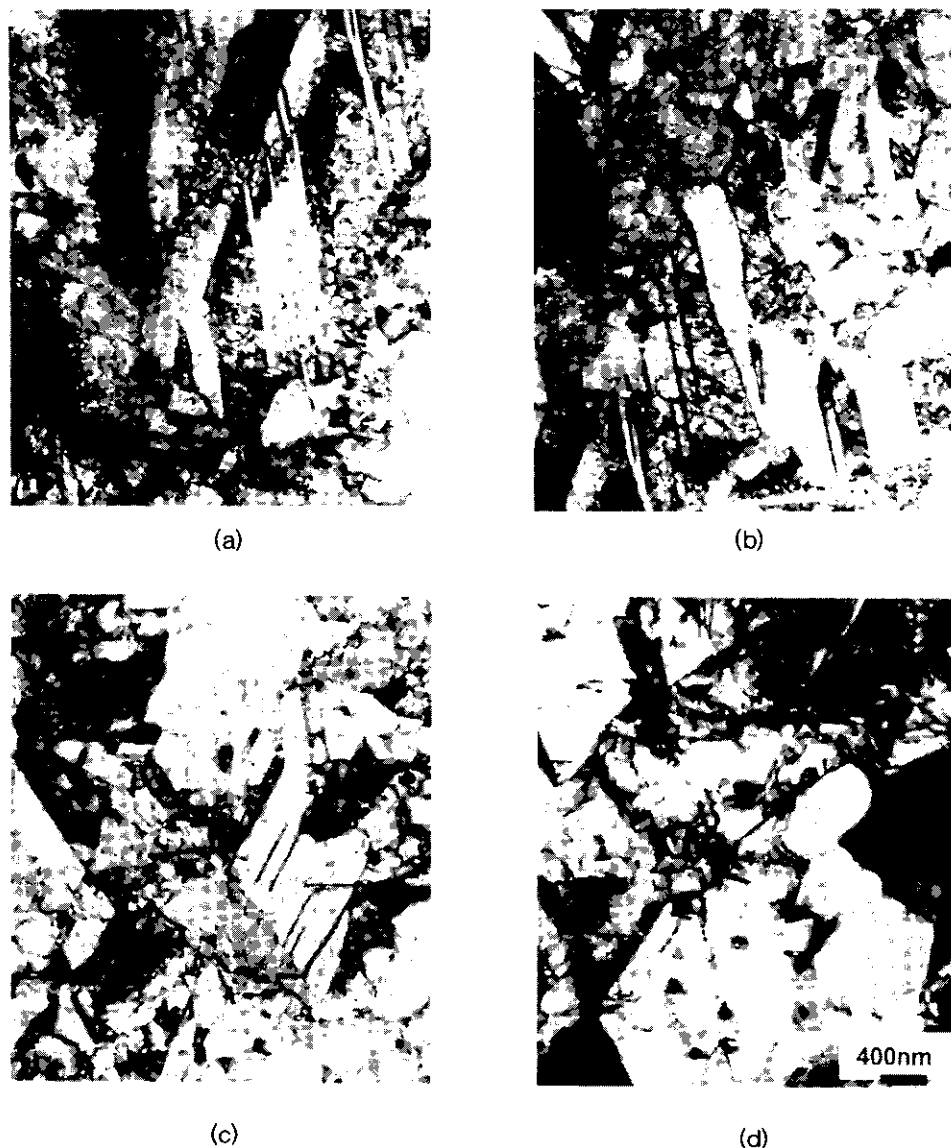


Fig. 5. Variations of microstructures of  $\beta$ -quenched Zr-1.5Sn alloy with annealing temperature (a) Room Temp. (b) 300°C (c) 550°C (d) 700°C

formation of precipitates from the supersaturated matrix. The coalescence of plates as well as the growth of precipitates were observed at 700°C, resulting in the sharp decrease of microhardness.

### 3.3. Recrystallization mechanisms for Zr-Sn alloys

It can be explained as follows that the process of recovery and recrystallization of the cold-worked alloys in the Fig. 1(a) is different from that of the  $\beta$ -quenched alloys in the Fig. 1(b). The cold-worked alloys have the dislocation network of cell structures in which dislocations are piled-up by the cold working. On the contrary, the  $\beta$ -quenched alloys do not form cell structures and disperse dislocations uniformly in the plates through the transformation of martensite. Since the uniformly dispersed dislocations can be moved more easily in general than those having cell structures in the

recovery process, the hardness of the  $\beta$ -quenched alloys has decreased by the recovery at 300°C while the hardness decrease of the cold-worked alloys delayed because it is harder to move the dislocation in the cold-worked alloys. By the way, the hardness of the cold-worked alloys decreased drastically by the recrystallization after recovery, but that of the  $\beta$ -quenched alloys increased again after recovery due to precipitation. In other words, many annealing processes were to be performed on the cold-worked alloys in manufacturing such as hot rolling at 700°C after  $\beta$ -quenching, annealing treatment at 700°C, cold rolling, annealing treatment at 610°C. Since the precipitates in the cold-worked alloys grew in the annealing processes, the additional precipitation could not progress at the annealing temperature below 700°C for recrystallization.

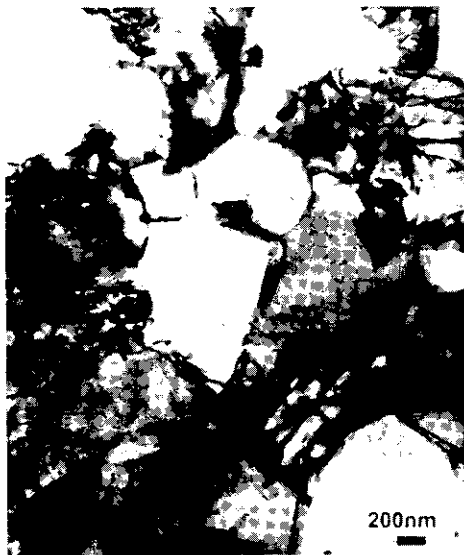


Fig. 6. TEM micrographs of cold-worked specimens showing the formation of a recrystallization nucleus by subgrain coalescence



Fig. 8. TEM micrograph of  $\beta$ -quenched specimen showing dislocation rearrangement as recrystallization progresses

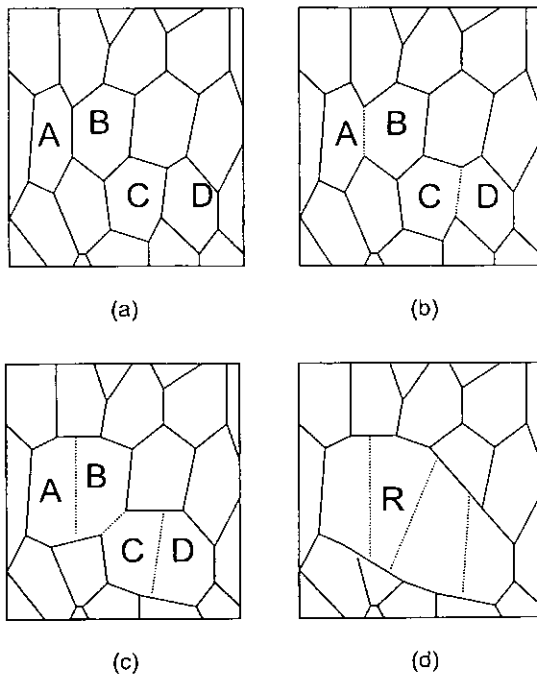


Fig. 7. Schematic representation of the formation of a recrystallization nucleus by subgrain coalescence<sup>9)</sup> (a) Subgrain structure before nucleation (b) Coalescence of subgrains A and B, and C and D (c) Further coalescence of subgrains B and C (d) Formation of a nucleus with high angle boundaries

The hardness of the  $\beta$ -quenched alloys also increased again because the additive elements in the supersaturated-solid solution formed precipitates through heat treatment at the temperature above 500 °C. Therefore, the recrystallization of cold-worked alloys behaved quite different from that of  $\beta$ -quenched alloys. A variety of mechanisms have been suggested to

explain the recrystallization process of alloys.<sup>4,7,8)</sup> In this study, the recrystallization mechanism for cold-worked Zr-Sn alloys is thought to be the subgrain coalescence. Recrystallization nuclei in the mechanism are originated by the subgrain coalescence. Fig. 6. Shows the coalescence of subgrains in the cold-worked matrix. A Stress-free grain was formed by the coalescence of subgrains and was used as a nucleus. Schematic diagrams explaining the formation of a recrystallization nucleus are indicated in Fig. 7.<sup>8)</sup> At the beginning, subgrains are randomly distributed in the matrix. Coalescence of subgrains progresses with the rearrangement of dislocations. Finally, a nucleus with high angle boundaries is created. In the meantime, the recrystallization mechanism for  $\beta$ -quenched specimens is quite different from that for the cold-worked sample.

In the quenched specimen, the dislocation structure was very inhomogeneous and the energy difference between the high energy grain and low energy grain is considered to be the driving force for the start of recrystallization.<sup>9)</sup> The observation of the massive grain growth suggests strain induced boundary migration<sup>10)</sup>, called "bulge nucleation" by Bailey and Hirsh.<sup>11)</sup> A bulge in a grain boundary surrounding material of low dislocation density migrates into the adjacent region if the dislocation density is higher. The condition for growth of a bulge is that the difference in strain energy per unit volume across the boundary is greater than the increase in grain boundary energy due to growth. Fig. 8 shows the stress-free area within a plate becoming wide as dislocations move to the grain boundaries.

#### 4. SUMMARY AND CONCLUSIONS

In Zr-Sn alloys the recrystallization of cold-worked specimens was completed between 500 and 600°C, while that of  $\beta$ -quenched samples did not start up to 600°C. This difference seems to happen because the stored energy of the  $\beta$ -quenched alloy for recrystallization is smaller than that of the cold-worked alloy. An increase of Sn content in Zr was also found to delay the recrystallization process of the Zr-Sn alloys. In the case of the  $\beta$ -quenched specimen precipitation was accompanied by the softening process during annealing, resulting in the increase of microhardness at a certain temperature range. Although the cold-worked and the  $\beta$ -quenched specimens had an equal initial hardness value, the recrystallization behaviors for those two cases were observed to be very different from each other. It is suggested that the recrystallization of the cold-worked sample would occur by the subgrain coalescence while that of the  $\beta$ -quenched sample would progress by the strain-induced grain boundary migration.

#### ACKNOWLEDGEMENTS

This project has been carried out under the nuclear

R&D program by MOST.

#### REFERENCES

1. IAEA, IAEA Report, TECDOC-996 (1998).
2. Y.H. Jeong and J.H. Baek, *J. of Corro. Sci. Soc. of Korea* **27**, 339 (1998).
3. Y.M. Yeon, Y.H. Jeong, and M.Y. Wee, *Korean J. of Materials Research* **7**(9), 772 (1997).
4. Jae-Song Koo, M.S. thesis, Dept. of Metallurgical Eng., Chungnam National University (1999).
5. N. Sano and K. Takeda, *J. of Nucl. Mater.* **252**, 63 (1998).
6. D. Charquet, R. Hahn, E. Ortlieb, J.P. Gros, and J.F. Wadier, *ASTM STP* **1023**, 405 (1988).
7. R.W. Cahn, *Proc. Phys. Soc.* **A64**, 324 (1950).
8. L. Himmel, *Proc. of a Symposium for Recovery and Recrystallization*, New York, **311** (1962).
9. W.M. Rumber and C.E. Coleman, *J. of Nucl. Mater.*, **36**, 147 (1970).
10. P.A. Beck and P.R. Sperry, *J. Appl. Phys.* **21**, 150 (1950).
11. J.E. Bailey and P.B. Hirsch, *Proc. Roy. Soc.* **267A**, 11 (1962).